

УДК 539.12

## THE DELPHI EXPERIMENT AT LEP

*G.D.Alexeev, D.Yu.Bardin, M.S.Bilenky, I.R.Boyko, G.A.Chelkov,  
L.V.Kalinovskaia, B.A.Khomenko, N.N.Khovanski, O.M.Kouznnetsov,  
Z.V.Krumstein, V.L.Malyshev, M.Yu.Nikolenko, A.G.Olchevski\*,  
V.N.Pozdniakov, N.E.Pukhaeva, A.B.Sadovsky, Y.V.Sedykh,  
A.N.Sissakian, O.G.Smirnova, L.G.Tkatchev, I.A.Tyapkin,  
L.S.Vertogradov, A.S.Vodopyanov, N.I.Zimin, A.I.Zintchenko*

This paper summarizes the current status of the DELPHI experiment, which is operating at the Large Electron Positron (LEP) Collider at CERN. The results from running at the energies around the  $Z$  resonance (LEP1) are based on the full available data, while the results obtained at higher energies (LEP2) are based on the data collected up to 1998. The analysis of the data collected at highest centre-of-mass energies (above 200 GeV) is still in progress and new results are expected. In this paper we present briefly some of the most important DELPHI results paying a special attention to the contribution of JINR group to the detector construction and data analysis.

The investigation has been performed at the Laboratory of Nuclear Problems, JINR.

## Эксперимент DELPHI на LEP

*Г.Д.Алексеев и др.*

В настоящей работе обсуждаются результаты, полученные на установке DELPHI, которая работает на большом электрон-позитронном коллайдере (LEP) в ЦЕРН. Для определения физических параметров при энергии в области  $Z$ -резонанса (LEP1) использовался весь имеющийся в распоряжении коллаборации набор данных, тогда как определение этих параметров при больших энергиях (LEP2) опирается на данные, полученные при еще больших значениях энергии (более 200 ГэВ), на их основе предполагается получить новые интересные результаты. В данной работе в краткой форме представлены только некоторые наиболее важные результаты эксперимента DELPHI, при этом особое внимание уделяется вкладу дубненской группы в создание детектора и анализ данных.

Работа выполнена в Лаборатории ядерных проблем ОИЯИ.

---

\*Leader from JINR

## INTRODUCTION

DELPHI is a general-purpose detector (Fig. 1) for physics at LEP on and above the  $Z^0$ , offering three-dimensional information on track curvature and particle energy deposition with fine spatial granularity as well as identification of leptons and hadrons over most of the solid angle. Detailed description of the detector and its performance can be found elsewhere [1].

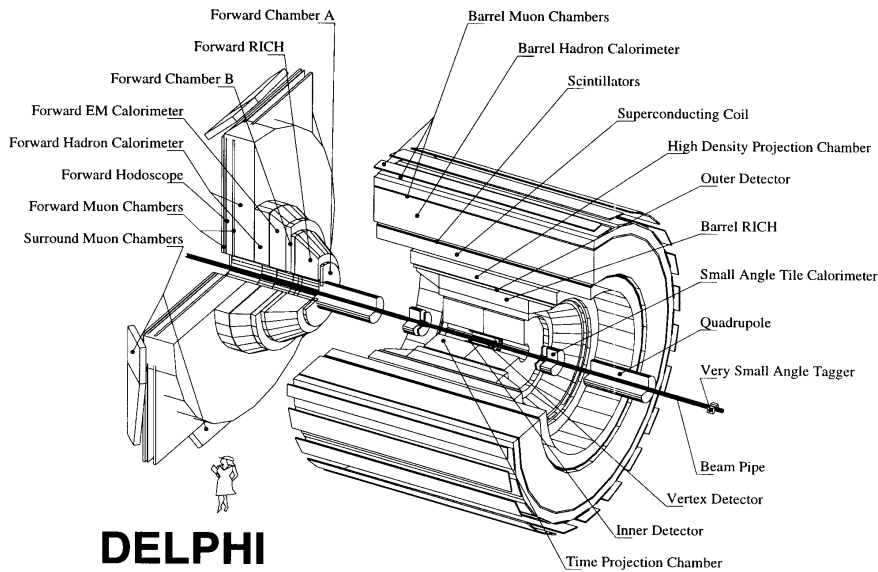


Fig. 1. The DELPHI detector at LEP

Since the startup of LEP in 1989, the luminosity of the collider was constantly increased from year to year so that the design parameters of the machine were exceeded. LEP has been operating at the energies around the  $Z$  resonance up to the year 1995 inclusively and, by that time, the DELPHI experiment collected statistics of about  $4.5 \cdot 10^6$   $Z$ -boson decays. This large statistics and high quality of the data allowed DELPHI to obtain a number of important results in electroweak theory, QCD, searches for new particles,  $b$ -quark physics and many others.

Since 1995 LEP is gradually increasing its energy and in 1998 about  $200 \text{ pb}^{-1}$  of integrated luminosity were delivered at 189 GeV, the energy, that is well above the threshold of  $W$ -pair production. In total, by the year 2000, LEP will provide about  $500 \text{ pb}^{-1}$  of integrated luminosity at the energies close to 200 GeV. This is giving new excellent possibilities in searching for new particles (in particular Higgs boson) and continuing the tests of electroweak theory, QCD, two-photon and other physics at a new level of precision.

One of the well known distinguished LEP results is the precise measurement of the  $Z$ -boson mass and total width, which became possible due to very precise calibration of the collision energy, high luminosity of the collider and excellent performance of detectors. With the LEP data, it became possible to obtain the information related to  $Z$  decays into invisible

channels and to measure the number of light neutrino species:  $N_\nu = 2.994 \pm 0.011$ . For the first time the presence of electroweak fermionic and bosonic corrections has been proven [2].

The new level of confidence in the Standard Model has been achieved when the top quark was discovered at Fermilab with the mass almost exactly predicted by the LEP data. Today, using the full list of electroweak measurements, including direct measurement of the top-quark mass, one can put constraints on the mass of the Higgs boson. The result of such analysis, which was performed by the LEP ElectroWeak Working Group, is shown in Fig. 2. The minimum of  $\chi^2$  corresponds to the mass of the Higgs boson:  $M_H = 76^{+85}_{-47}$  GeV [2].

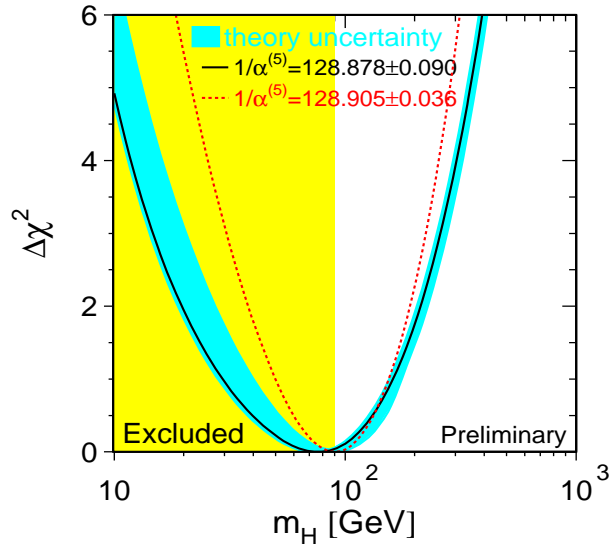


Fig. 2. Indirect measurement of the Higgs boson at LEP

While electroweak measurements provide indirect constraints on the mass of the Higgs boson, direct searches performed at LEP pushed the lower limit of the Standard-Model Higgs boson mass. As is typical in searches, the statistics at the highest possible collider energy is more important and, at present, the best limit  $M_H > 94.1$  GeV was obtained from the preliminary analysis of the 1998 DELPHI data collected at 189 GeV [3].

In Fig. 3 it is shown that the interpretation of these high-energy data together with the theoretical constraints in the Supersymmetric extension of the Standard Model for the first time started to exclude completely the region of small  $\tan\beta$  [3].

The subject of QCD studies at LEP deserves special attention. Different analyses in this area profit from high statistics of events with hadronic final state and well-understood performance of the detectors. From the analysis of 4-jet hadronic events DELPHI has proved one of the basic QCD features — the gluon self-coupling — and measured the number of gluons, which exist in nature:  $N_g = 8 \pm 2$  [4].

Using the data taken by DELPHI at different LEP energies the evolution of different QCD parameters has been studied. In particular, the value of the  $b$ -quark mass at the  $M_Z$

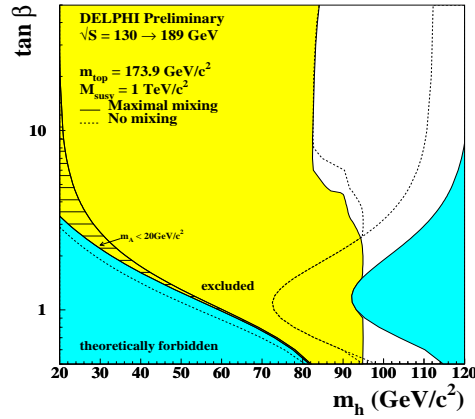
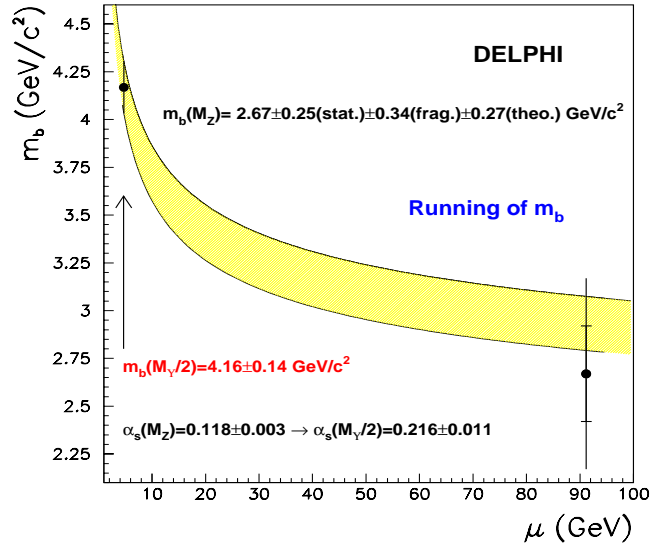


Fig. 3. Exclusion limits of SUSY parameters

Fig. 4. DELPHI measurement of running  $m_b$ 

scale  $m_b(M_Z) = 2.67 \pm 0.50 \text{ GeV}/c^2$  was determined, which agrees with the QCD prediction of having a running  $b$ -quark mass. This result is demonstrated in Fig. 4. The study also verified the flavour independence of the strong coupling constant for  $b$  and light quarks within 1% accuracy [5].

By now, DELPHI results from running at  $Z$  resonance and at LEP200 are summarized in about 200 papers and it is impossible to give here even a brief description of all of them. In

the following we, therefore, will restrict ourselves to the main results, where the contribution from the Dubna group members was essential. The description starts with the hardware contribution and continues with the results of the data analyses.

## PERFORMANCE OF THE HCAL AND SMC

In this section we briefly overview the performance of two DELPHI subdetectors, the Hadron CALorimeter (HCAL) and the Surround Muon Chambers (SMC), which were constructed and operated with a significant contribution of the Dubna group.

The iron return yoke of the DELPHI magnet is instrumented with plastic streamer tube (PST) detectors to create a sampling gas calorimeter, the HCAL. The pad readout system for the measurement of energy deposition was operating since the very beginning of DELPHI experiment.

In addition, in 1995–1996 a system to read out the cathodes of individual tubes (CRO) was implemented. The CRO system is independent of pad readout and improves the granularity in  $\phi$  by a factor of 3 and in R by a factor of 5. The combination of two readout systems provides better  $\pi/\mu$  separation, improved detection of neutral particles, enhanced discrimination between neighboring showers and more precise hadron energy measurement.

Yet another system — readout of the anodes of tubes (ARO) — used for timing (resolution about 20 ns) and triggering purposes was commissioned in 1997/1998 for inner HCAL layers. All layers will be equipped with ARO for the 1999 data taking.

An excellent performance of all three HCAL readouts allowed DELPHI to participate in *COSMOLEP* — the project to study cosmic events with LEP detectors. In Fig. 5 a *COSMOLEP* event from the test data taking in 1998 is shown. It was triggered by the anode readout and the tracks were reconstructed with pad and cathode readouts.

During the years of DELPHI operation the HCAL has proven to be very stable, efficient and reliable.

In 1994 the Surround Muon Chambers based on detectors similar to the HCAL PST's were installed outside the endcaps to fill the gap between the barrel and forward DELPHI muon systems. That improved the hermiticity of the muon identification (Fig. 6 and, in total, SMC demonstrated robust and reliable performance, with less than 1% losses of the detector units over five years of operation.

## LEP1 RESULTS

**Electroweak Physics.** The sensitivity in electroweak observables achieved experimentally after the years of LEP operation at the energies around the  $Z$  resonance requires the highest standards on the theoretical side as well.

One of the most popular and powerful theoretical tools used for the data interpretation is the ZFITTER package [6]. Based on semi-analytic calculations performed in the framework of the Standard Model, it provides an accuracy of typically  $\sim 0.01\%$ , which required an account of all known higher-order QED, electroweak and QCD results. The present accuracy

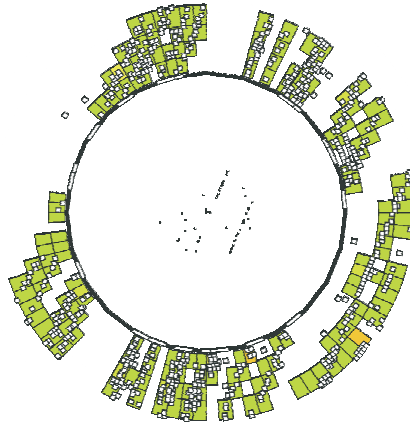
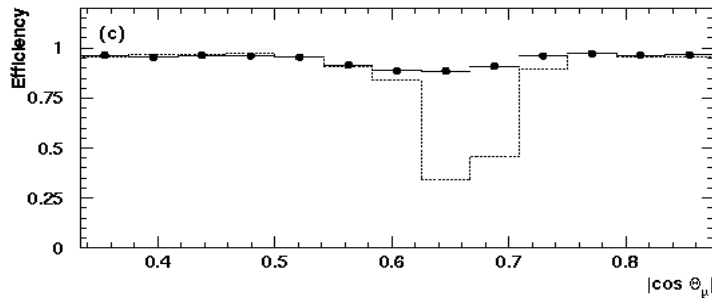
Fig. 5. R- $\phi$  view of a typical COSMOLEP event

Fig. 6. DELPHI muon identification efficiency versus the polar angle before (line) and after (points) installation of the SMC

of the theory and its importance are well demonstrated in Fig. 2, where the width of the band around the  $\chi^2$  curve represents the uncertainty due to different theoretical sources.

Calculation of two-fermion standard processes remains important at LEP2 as well. In addition, for the data analysis at these high energies, another theoretical contribution has been made — the semi-analytic program GENTLE [7], which calculates the  $W$ -pair production cross section and provides a benchmark for different Monte-Carlo generators.

*$Z^0$  Lineshape Measurement.* The study of fermion-antifermion pair production in  $e^+e^-$  collisions at LEP1 energies (around 91 GeV) is the most powerful tool for determining the parameters of the Standard Model and for checking its consistency. The experimentally measured quantities are cross sections of hadronic and leptonic final states, charge forward-backward asymmetries and fermion polarizations.

The hadronic final state profits from the high precision of the cross section measurement due to the large statistics of selected events and careful analysis of systematic uncertainties. Almost 4 000 000 hadronic decays of  $Z$  boson were collected with the DELPHI detector during the LEP1 run from 1989 to 1995.

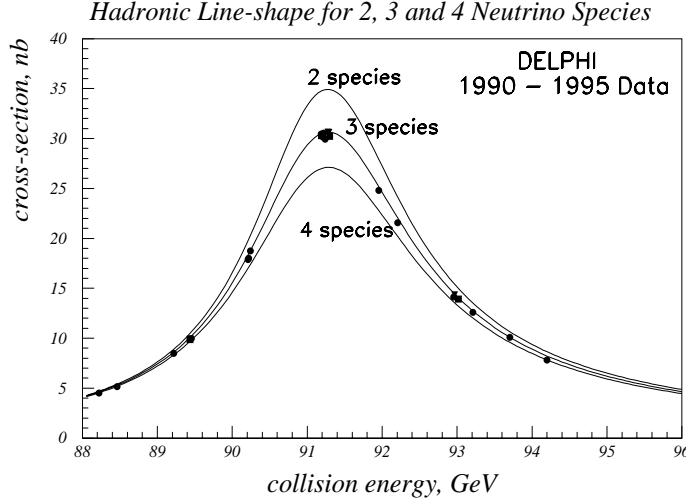


Fig. 7. Hadronic line-shape for 2,3 and 4 neutrino species. The points are based on the data collected by DELPHI at LEP1

Their distinctive feature is a large number of primary charged tracks, which allows efficient selection of the signal events with very low background.

The main selection criteria used in the analysis are: the charged multiplicity  $N_{\text{ch}} > 4$  and the charged energy  $E_{\text{ch}} > 0.12\sqrt{s}$ . This gives a signal selection efficiency of about 95% and a residual background of about 0.5%.

The resulting statistical and systematic uncertainties for the cross sections amount to few promille. The measured hadronic cross section is presented in Fig. 7 as a function of LEP energy. In this plot the Standard Model prediction for the number of light neutrino species equal to 2, 3 and 4 is also shown. The data clearly favour  $N_{\nu} = 3$ .

The leptonic final states comprising only 15% of the visible  $Z^0$  cross section also provide important information for the global electroweak fit. As an example of a leptonic final state analysis the most complex channel,  $ee \rightarrow Z^0 \rightarrow \tau\tau$ , is presented here.

The analysis is restricted to the  $20^\circ < \theta < 160^\circ$  range of polar angles where the best detector performance is achieved. The events are selected as two low-multiplicity back-to-back jets thus rejecting the background from  $Z^0 \rightarrow qq$  and two-photon collisions.

The background from non-tau  $Z^0$  leptonic decays is rejected by kinematic cuts, which ensure that the track momenta and electromagnetic energies are incompatible with  $Z^0 \rightarrow ee$  or  $Z^0 \rightarrow \mu\mu$ . The resultant selection efficiency is about 62% and the residual background is close to 3%.

In addition to the measurement of the cross section, the charge forward-backward asymmetry is determined from the azimuthal angle distribution of the negative lepton.

In Fig.8 the measured asymmetry and its energy evolution are clearly seen. The total systematic error for the tau cross section measurement was 0.6% while for the asymmetry it was 0.002.

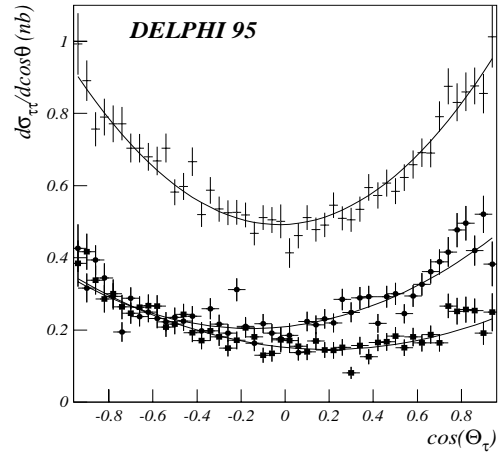


Fig. 8. Angular differential cross section of negative tau production. Squares, crosses and circles stand for LEP energies 89.438 GeV, 91.278 GeV and 92.965 GeV, respectively

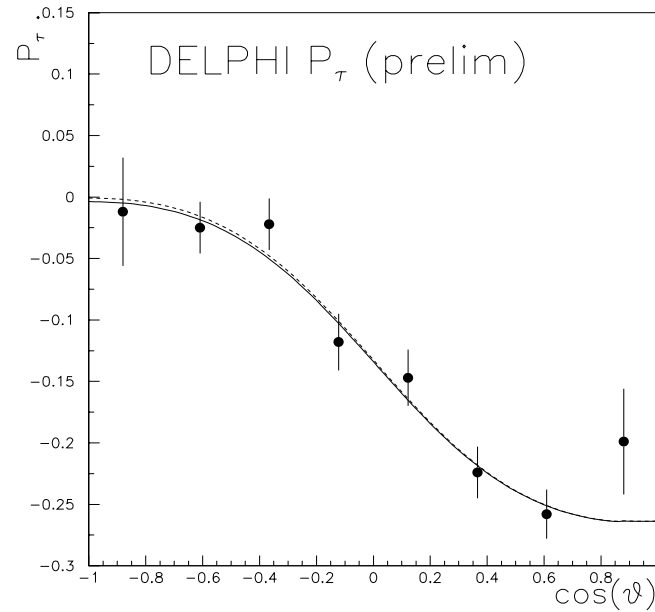


Fig. 9. Tau polarization as a function of the negative tau direction

All the results on the fermion pair production [8] at LEP1 were found to be in agreement with the Standard Model predictions.

*Electroweak Properties of  $\tau$  Decays.* Additional information on the Standard Model parameters can be extracted from the polarization of the final state fermions.

At LEP energies only the tau lepton polarization can be measured, from the spectra of  $\tau$  decay products. The polarization is determined separately for each major tau decay mode, these are identified by electromagnetic and hadron calorimeters and muon chambers. The value of polarization is extracted by comparing the experimental spectra with the Monte-Carlo predictions for decays of left- and right-handed taus. Additional information is extracted from the polarization forward-backward asymmetry (Fig. 9). The combination of results [9] allows one to measure the electroweak parameter  $A_l = 0.1369 \pm 0.0065 \pm 0.0043$ , or, equivalently  $\sin^2\theta_W = 0.23288 \pm 0.00097$ .

The study of the tau decay spectra allows additional checks of the Standard Model in the charged current sector. In [10] the measurement of the Michel parameters from tau decays is described. All the measured parameters are in agreement with the Standard Model. A new type of tensor interaction was also tested and its contribution was found to be consistent with zero. Therefore, an upper limit on the strength of the tensor interaction has been set.

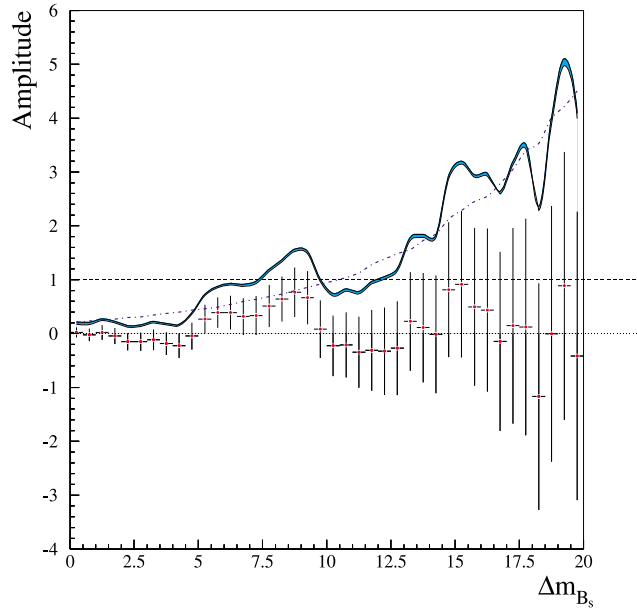


Fig. 10. Oscillation amplitude  $A$  (the error bars) as a function of  $\Delta m_{B_s}$ .

**Study of  $B_s^0 - \bar{B}_s^0$  Oscillations.** The large samples of events accumulated by LEP experiments and the relatively high purity and efficiency of  $b$ -tagging allowed different B-physics studies. Among them the precise determination of the values of the  $\rho$  and  $\eta$  parameters (in terms of the Wolfenstein parameterization) of the  $V_{CKM}$  matrix elements is one of the most interesting. Several quantities which depend on  $\rho$  and  $\eta$  can be measured and, if the Standard Model is correct, they must define compatible values for the two parameters, within measurement errors and theoretical uncertainties. Among these important quantities are the mass differences between CP eigenstates  $\Delta m_{B_d}$  and  $\Delta m_{B_s}$  in the neutral B mesons. Several

experimental methods have been used [11] by DELPHI to study  $B_s^0 - \overline{B}_s^0$  oscillations. One of them — using exclusive  $B_s$  — has been pioneered recently and, despite the small statistics, gives an important contribution to the high  $\Delta m_{B_s}$  mass region, due to the excellent proper time resolution.

The combined DELPHI result with the relevant explanations is shown in Fig. 10. The combined world result gives the upper limit  $\Delta m_{B_s} > 12.4 \text{ ps}^{-1}$  at 95% C.L. with a sensitivity of  $13.8 \text{ ps}^{-1}$  and is defined mainly by the results from two LEP experiments: ALEPH and DELPHI. The limit obtained gave an important impact on the  $\rho = 0.189 \pm 0.074$  and  $\eta = 0.354 \pm 0.045$  determination [12]. On the other hand, from quantities depending on  $\rho$  and  $\eta$  the expected value of  $\Delta m_{B_s}$  at 95% C.L. can be estimated [12]:  $5 \text{ ps}^{-1} < \Delta m_{B_s} < 21 \text{ ps}^{-1}$ . The present limit covers about half of this region.

**Experimental Study of Different QCD Effects.** The data collected by DELPHI have been used to measure the transverse  $F_T$  and longitudinal  $F_L$  fragmentation functions, which were evaluated from the double differential charged hadron cross section  $\frac{d^2\sigma^{\text{ch}}}{dx_p d\cos\theta}$ . Confirming theoretical predictions,  $F_L$  was found to be nonzero in the region of  $x_p < 0.2$  and vanishing at higher  $x_p$  (Fig. 11).

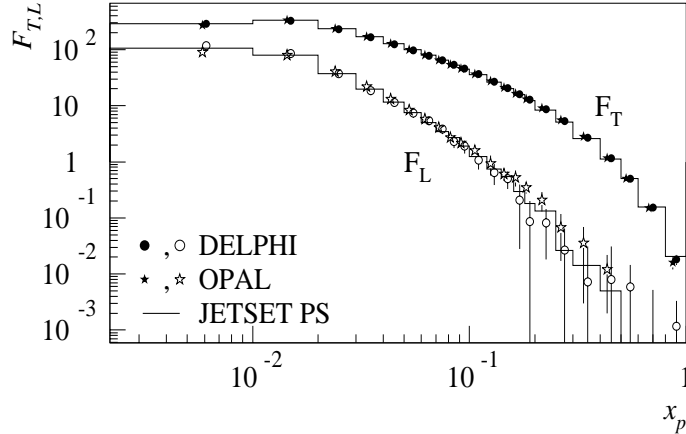


Fig. 11. Measured values of  $F_L$  and  $F_T$  obtained in DELPHI (circles). Also shown are OPAL data (stars) and Monte-Carlo distributions (histograms)

Using the first moments of the measured fragmentation functions, the mean charged multiplicity in  $Z^0$  hadronic decays was found to be  $\langle n^{ch} \rangle = 21.21 \pm 0.20$ . The second moments of  $F_T$  and  $F_L$  were used to calculate the strong coupling constant  $\alpha_s(M_Z)$  in the next-to-leading order of perturbative QCD, giving  $\alpha_s^{\text{NLO}}(M_Z) = 0.120 \pm 0.013$ . Inclusion of nonperturbative power corrections led to the value of  $\alpha_s^{\text{NLO+POW}}(M_Z) = 0.101 \pm 0.013$ . For further details, see [13].

The first probe of the correlation of the T-odd one-particle fragmentation function, which is responsible for the left-right asymmetry of fragmentation of a transversely polarized quark, has been done with the DELPHI data for  $Z^0 \rightarrow 2$  jets decays.

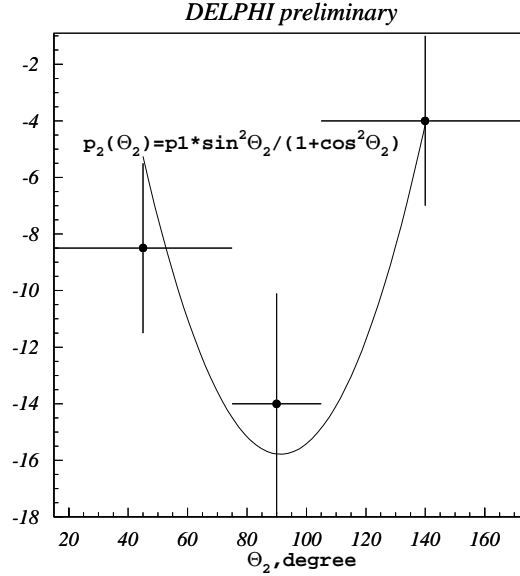


Fig. 12. The polar angle dependence of the azimuthal correlation (in ppm) of leading hadrons in back-to-back jets

Though the transverse polarization of a quark in  $Z^0$  decay is very small ( $O(m_q/M_Z)$ ), there is a nontrivial *correlation* between transverse spins of a quark and an antiquark in the Standard Model:  $\overline{C_{TT}} \approx -0.5$  for the average over flavors.

This results in specific azimuthal asymmetry of the leading hadron produced in one jet around the direction of the leading hadron in the second jet:

$$\frac{d\sigma}{d\cos\theta_2 d\phi_1} \propto 1 + \frac{6}{\pi} S^2 \overline{C_{TT}} \frac{\sin^2\theta_2}{1 + \cos^2\theta_2} \cos(2\phi_1),$$

where  $\theta_2$  is the polar angle of the second hadron with respect to the beam axis and the azimuthal angle of the first hadron,  $\phi_1$ , is defined relatively to the plane of the beam and second hadron. The experimental result and the best fit for the coefficient of  $\cos(2\phi_1)$  are shown in Fig. 12 and correspond to the value of analyzing power:  $|S| = 12.9 \pm 1.4\%$  [14].

## LEP2 PHYSICS

**Fermion Pair Production.** The study of  $e^+e^- \rightarrow f\bar{f}(\gamma)$  production at LEP2 has two purposes: to provide a new input for constraining theory parameters and to look for possible deviations from the Standard Model predictions at high collision energies. A typical feature of events at LEP2 is strong Initial State Radiation of photons, which brings the effective (or «reduced») collision energy ( $\sqrt{s'}$ ) from the nominal centre-of-mass energy of LEP ( $\sqrt{s}$ ) down to the  $Z^0$ . Therefore the cross sections and leptonic asymmetries can be determined for different ranges of  $\sqrt{s'}$ .

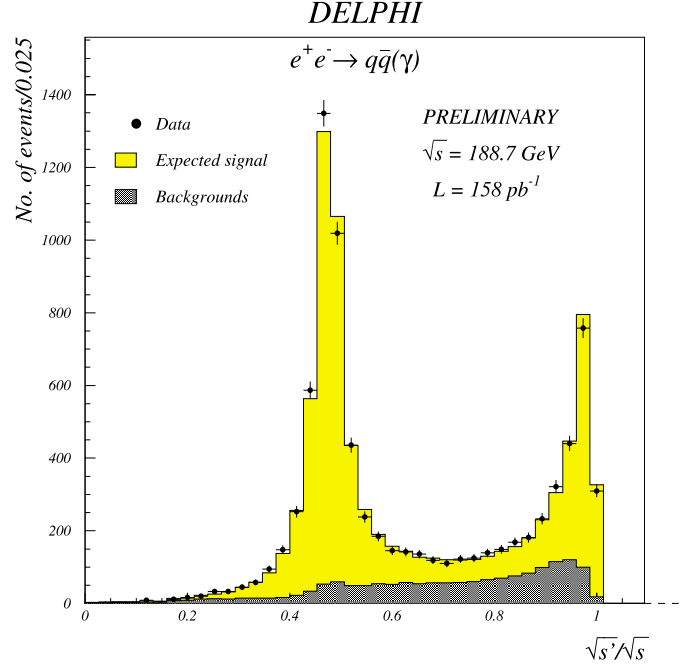


Fig. 13. Reconstruction reduced energy distribution based on hadronic events collected at 189 GeV collision energy

In practice, the «inclusive» values are measured for the range  $\sqrt{s'}/\sqrt{s} > 0.1$  (multihadronic events) or  $\sqrt{s'} > 75 \text{ GeV}$  (leptonic events) and the «non-radiative» values for the range  $\sqrt{s'}/\sqrt{s} > 0.85$ . The nonradiative measurements should be more sensitive to the manifestations of new physics phenomena. The distribution of reconstructed reduced energy for multihadronic events is shown in Fig. 13.

The hadronic event selection in the analysis of the LEP2 data is very similar to the one of the LEP1 analysis (see LEP1 section) with the cuts  $N_{\text{ch}} > 6$  and  $E_{\text{ch}} > 0.15 \sqrt{s}$ . The selection efficiency in this case is about 85% and the residual background is of the order of 20%. The dominant background comes from the  $e^+e^- \rightarrow W^+W^-$  process.

In the case of the  $ee \rightarrow \tau\tau$  process most of the selection cuts used at LEP1 were tightened in order to achieve much larger suppression of Bhabha and two-photon background.

The two jets were required to be coplanar with the beam axis instead of back-to-back topology at LEP1. The signal selection efficiency was about 50% and the residual background was about 13%.

The high-energy data sample accumulated by DELPHI during three years 1996–1998, corresponding to about  $240 \text{ pb}^{-1}$  of integrated luminosity collected at 130–189 GeV of LEP energies, was analyzed to determine the cross sections and leptonic forward-backward asymmetries.

The energy evolution of hadronic and leptonic cross sections can be seen in Fig. 14. No significant deviations from the Standard Model predictions were found and limits were set on the parameters of different models with additional  $Z'$  bosons, contact interactions between fermions and others. Preliminary numbers were reported at the conferences [15].

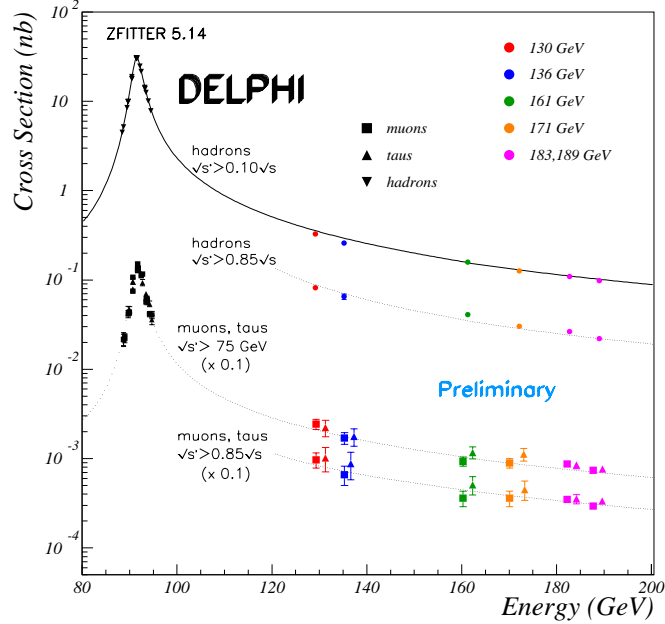


Fig. 14. Fermion pair production cross section at LEP1 and LEP2

**$W$  Pair Production.** One of the main goals of LEP2 is to perform a precision, down to  $\sim 40$  MeV, measurement of the  $W$  mass, which requires the use of all possible  $W$  decay channels in the analysis. The distribution of the reconstructed  $W$  mass in the  $WW \rightarrow q\bar{q}q\bar{q}$  channel is shown in Fig. 15 [16].

This channel is the most statistically powerful but the mass reconstruction in it is likely to be affected by the final state interaction between the hadrons from different  $W$ 's — Bose–Einstein correlations and colour reconnection. Potentially, those effects can be large, because the typical separation between the  $W^+$  and  $W^-$  in  $e^+e^- \rightarrow W^+W^-$  events at LEP2 energies is small,  $\sim 0.1$  fm.

At the present level of statistics, however, the experimental data (Fig. 16) show no evidence for Bose–Einstein correlations in the correlation function  $R(Q)$  for like-sign particles arising from different  $W$ 's measured at 172 GeV [17]. A preliminary analysis of the 183 GeV data shows the same tendency [18].

Possible effects of interference due to colour reconnection in hadronic decays of  $W$  pairs also have been studied from the data [19], but these studies were statistically limited. With  $500 \text{ pb}^{-1}$  of integrated luminosity planned for LEP2, it should be possible to get more definite results on both effects.

## $\gamma\gamma$ -PHYSICS

**Photon Structure Function Study.** One of the main interests in the  $\gamma\gamma$  physics is an understanding of the photon structure function behaviour in the wide region of  $Q^2$  and  $x$ . Such

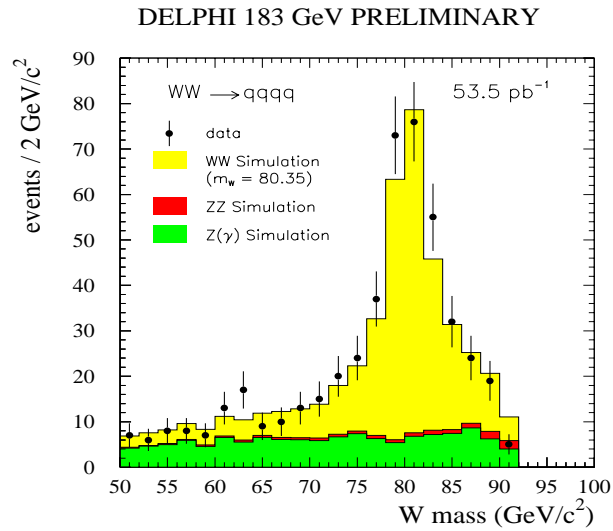


Fig. 15. Reconstructed  $W$  mass for the  $WW \rightarrow q\bar{q}q\bar{q}$  candidates (only one mass per event)

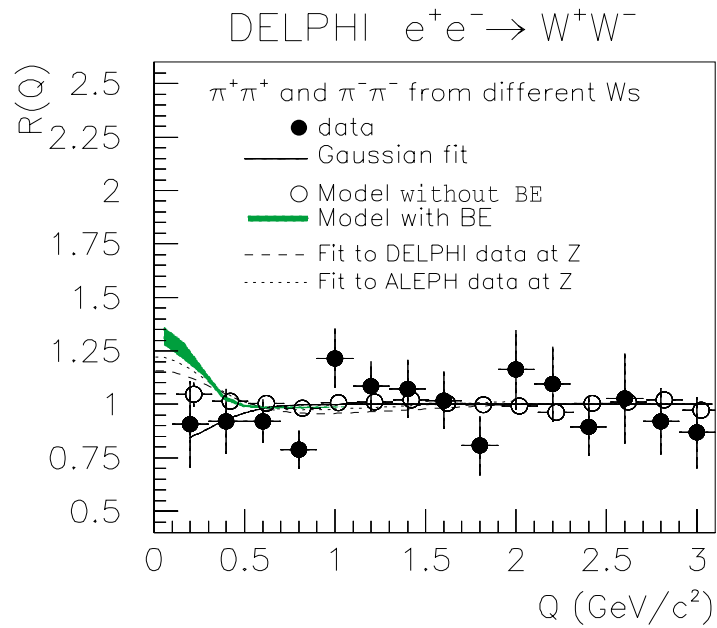


Fig. 16. The correlation function for data (closed circles) and simulation without BE symmetrization (open circles)

study will throw light on the parton distributions in the photon, which should be determined experimentally as an input to the perturbative QCD and soft nonperturbative interactions. The photon structure function can be measured in the reaction  $e^+e^- \rightarrow e^+e^-\gamma\gamma^* \rightarrow e^+e^-X$ , where  $X$  is a multihadronic system and one of the scattered leptons is observed at a large scattering angle (tagging condition) while the other, remaining at a small angle, is undetected (antitagging condition). Here  $\gamma$  is an almost real photon which is probed by the virtual one,  $\gamma^*$ , and such a reaction is often called Deep Inelastic Scattering (DIS).

The corresponding cross section can be expressed in terms of the photon structure functions  $F_2^\gamma(x, Q^2)$  and  $F_L(x, Q^2)$ . Several types of physical process contribute to the total cross section: the point-like coupling of the photons to a quark-antiquark pair (QPM), the vector meson contribution (VDM) and the resolved photon contribution [20] (RPC), which was first proposed to be used in DIS by DELPHI [21]. At present, the main goal is to extend the study with the proposed three-component description of DIS to a wider  $Q^2$  region on the basis of LEP2 data. Our latest results for  $F_2^\gamma(x, Q^2)$  [22] are shown in Figs. 17,18.

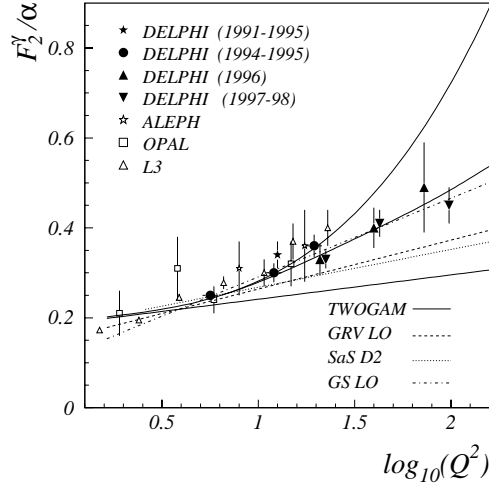
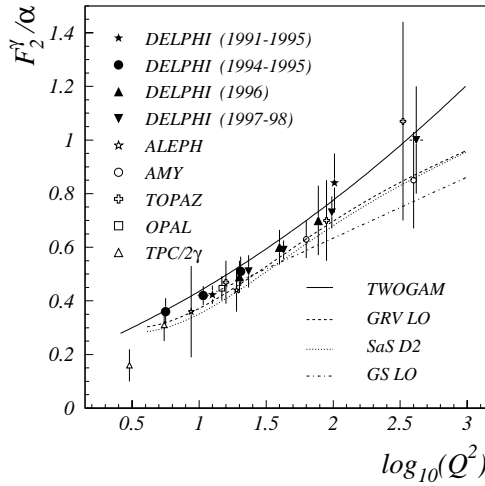


Fig. 17.  $F_2^\gamma$  versus  $\log(Q^2)$  for  $0.3 < x < 0.8$       Fig. 18.  $F_2^\gamma$  versus  $\log(Q^2)$  for  $0.01 < x < 0.1$

**Prospects for  $\gamma\gamma$  Physics with the DELPHI VSAT Detector.** Studies of  $\gamma\gamma$  collisions at LEP2 at very low momentum transfer  $Q^2$  measured by the Very Small Angle Tagger (VSAT) promise to bring new interesting results:

- for single tagged events, where the power to distinguish between different models predicting quark and gluon densities inside the photon will be increased
- for double tagged events, when both scattered leptons are detected, cross section and virtual photon structure function will be measured in a very clean kinematic environment.

During the 1997–1998 shutdown period a smaller beam pipe was installed at the position of the VSAT calorimeters. This upgrade was initiated by the Dubna and Lund University

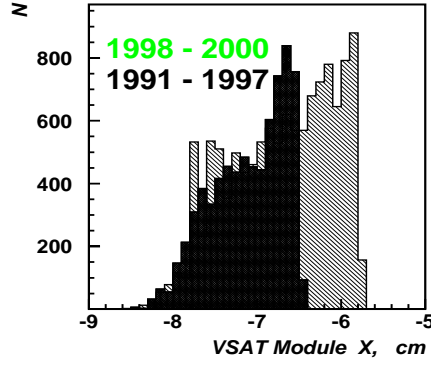


Fig. 19. New and old acceptance of the modules of the DELPHI VSAT detector

groups in order to increase the VSAT acceptance. Preliminary analysis of the 1998 data [23] shows the benefit of a factor of  $\simeq 2$  for double tagged and a factor of  $\simeq 1.5$  for single tagged events (Fig. 19).

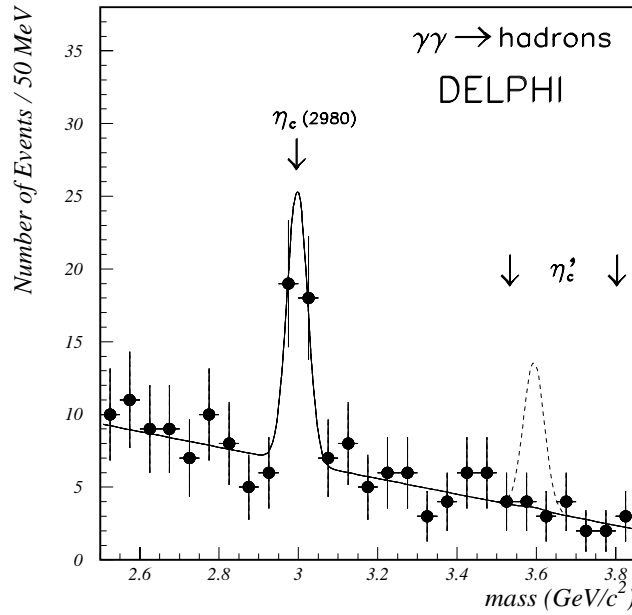


Fig. 20. Invariant mass distribution

**Production of  $\eta_c$  Mesons in Two-Photon Interactions.** The study of hadronic resonances produced in collisions of quasi-real photons has several advantages compared to the production in  $e^+e^-$  annihilation. A resonance can be produced alone, making the study simpler, since

there is no additional hadronic accompaniment in the reaction, and the production cross section of such process can be calculated in QED with only one parameter — the two-photon width of the resonance.

The LEP experimental conditions allow studies in the hadronic resonance mass domain up to  $2 \div 3$  GeV. Based on the data collected with the DELPHI detector, the production of  $\eta_c$  mesons in  $\gamma\gamma$  collisions has been studied. This analysis uses several decay modes of the resonances into charged pions and kaons and benefits from the advanced particle identification capabilities of DELPHI. The resulting invariant mass distribution is shown in Fig. 20. From the analysis of the data the  $\eta_c \rightarrow \gamma\gamma$  partial width has been measured [24] and the limit for the production of  $\eta'_c$  in  $\gamma\gamma$  collisions has been set [25].

### References

1. DELPHI Coll. — NIM, 1996, v.A378, p.57.
2. Karlen D. — Plenary Talk at ICHEP'98.
3. Ruhlmann-Kleider V. — DELPHI report to the LEPC, 12 Nov. 1998, CERN, Geneva.
4. DELPHI Coll. — Phys. Lett., 1997, v.B414, p.401.
5. DELPHI Coll. — Phys. Lett., 1998, v.B418, p.430.
6. Bardin D. et al. — Prepr. CERN TH 6443, 1992.
7. Bardin D. et al. — Phys. Lett., 1993, v.B308, p.403.
8. DELPHI Coll. — ICHEP'98 CONF # 438.
9. DELPHI Coll. — ICHEP'98 CONF # 243.
10. DELPHI Coll. — ICHEP'98 CONF # 244.
11. DELPHI Coll. — ICHEP'98 CONF # 235, # 236, # 237.
12. DELPHI Coll. — ICHEP'98 CONF # 586.
13. DELPHI Coll. — E. Phys.J., 1999, v.C6, p.19.
14. Tkatchev L., DELPHI Coll. — Proc. of SPIN98 Symp., Protvino, 1998.
15. DELPHI Coll. — ICHEP'98 CONF # 155, # 441, # 202.
16. DELPHI Coll. — ICHEP'98 CONF # 341.
17. DELPHI Coll. — Phys. Lett. B401 (1997) 181.
18. DELPHI Coll. — ICHEP'98 CONF # 288.
19. Pukhaeva N., DELPHI Coll. — Proc. ISMD' 97 Conf., Frascati. 8-12 Sept., 1997;  
DELPHI Coll. — ICHEP'98 CONF # 287.

20. DELPHI Coll. — *Z. Phys.*, 1994, v.C62, p.3.
21. Tyapkin I., DELPHI Coll. — ICHEP'96, Warsaw, 1996.
22. Tyapkin I., DELPHI Coll. — Proc. Photon'97 Conf., Egmond aan Zee, 1997; Proc. Workshop on Two-Photon Interactions, Lund. 10-13 Sept., 1998.
23. N.Zimin, DELPHI Coll. — Proc. Workshop on Two-Photon Interactions, Lund. 10-13 Sept., 1998.
24. DELPHI Coll. — ICHEP'98 CONF # 155.
25. DELPHI Coll. — CERN EP 98-151.

Received on February 1, 2000.